

# The chemical mechanism of exhaust gas recirculation on polycyclic aromatic hydrocarbons formation based on LIF measurement

Peng Liu<sup>a</sup>, Yiran Zhang<sup>a</sup>, Lijun Wang<sup>a</sup>, Bo Tian<sup>b</sup>, Bin Guan<sup>a</sup>, Dong Han<sup>a</sup>, Zhen Huang<sup>a</sup>, He Lin<sup>a</sup>

<sup>a</sup>Key Laboratory for Power Machinery and Engineering of Ministry of Education, School of Mechanical Engineering,

Shanghai Jiao Tong University, Shanghai 200240, China

<sup>b</sup>Department of Engineering, University of Cambridge, CB21PZ, Cambridge, UK

## 1. The details of time resolved LII intensity calculation

In order to eliminate the bias caused by the evolution of LII signal. A simulation of time resolved LII signal has been performed. The well-known energy balance model for LII after energy absorption, originally formulated by Melton [1] and subsequently refined by a number of researchers over the years [2–4], includes heat addition by the laser pulse and various cooling terms in the general form:

$$\frac{dU_{in}}{dt} = \dot{Q}_a - \dot{Q}_s - \dot{Q}_c - \dot{Q}_r \quad (1)$$

where  $U_{in}$ ,  $\dot{Q}_a$ ,  $\dot{Q}_s$ ,  $\dot{Q}_c$  and  $\dot{Q}_r$  represent, respectively, the internal energy, the laser energy absorption rate, the sublimation rate of carbonaceous materials, the rate of heat loss via thermal conduction and the rate of heat loss via thermal radiation. The rate of change in internal energy of a spherical primary particle can be expressed as:

$$\frac{dU_{in}}{dt} = \rho_s c_s \frac{\pi}{6} D^3 \frac{dT}{dt} \quad (2)$$

where the values of density  $\rho_s$  and specific heat capacity  $c_s$  can be found in table 1. The absorption term  $\dot{Q}_a$  is given with Eq. (3)

$$\dot{Q}_a = \frac{\pi^2 D^3 E(m)}{\lambda_l} \cdot \frac{Fq(t)}{q_{\max}} \quad (3)$$

where  $F$  is the fluence of laser beam/sheet with the unit of  $J/m^2$ ,  $q(t)$  is the temporal profile of laser pulse,  $q_{\max}$  is a constant used to normalize the integrated laser temporal profile to unity,  $\lambda_l$  is the laser wavelength, and  $E(m)$  is the absorption function of soot at certain  $\lambda_l$ . In the present study, the value of  $E(m)$  is problematic since  $\lambda_l$  is 266 nm, which is not a normally used wavelength to conduct LII measurements. Therefore, there is few value of  $E(m)$  under this wavelength was reported. Here we use the experimental data for  $E(m)$  of Krishnan et al. [5] and a linear fitting by Snelling et al. [6] to estimate the value at 266 nm, which is:

$$E(m) = 0.232 + \lambda \cdot (1.2546 \times 10^5 \text{ m}^{-1}) \quad (4)$$

The calculations of the heat loss rate via conduction  $\dot{Q}_c$ , sublimation  $\dot{Q}_s$  and radiation  $\dot{Q}_r$  are based on the fully constrained model summarized by Michelsen et al. [3,4] as Eqs. (5-7):

$$\dot{Q}_c = \frac{2k_a \pi D^2}{D + GL_{\text{MFP}}} (T - T_g) \quad (5)$$

where  $T_g$  is the temperature of the ambient gases,  $k_a$  is the thermal conductivity of the surrounding gases,

and  $L_{\text{MFP}}$  is the mean free path. The heat transfer factor  $G$  is given by  $G = \frac{8f}{\alpha_T(\gamma + 1)}$ , where  $\alpha_T$  is the thermal accommodation coefficient;  $\gamma$  is the heat capacity ratio for air; and  $f$  is the Eucken correction to the thermal conductivity given by:  $f = \frac{9\gamma - 5}{4}$ .

Sublimation is an endothermic phase transition process. Heat loss by sublimation is modeled as:

$$\dot{Q}_s = -\frac{\Delta H_v}{W_s} \frac{dM}{dt} = \frac{\Delta H_v}{W_s} \frac{\pi W_v \alpha_M P_v}{R_g T} \left( \frac{R_g T}{2W_v} \right)^{\frac{1}{2}} \quad (6)$$

where  $W_s$  is the molecular weight of solid carbon, and  $\Delta H_v$  is the enthalpy of formation of sublimed carbon clusters;  $\alpha_M$  is the mass accommodation coefficient, which is taken as unity in the present study [1,7];  $R_g$  is the universal gas constant;  $W_v$  is the molecule weight of C3, which is assumed as main composition of vaped cluster of carbon;  $P_v$  is the partial pressure of sublimed carbon clusters C3, and is given by the Clausius-Clapeyron equation:  $P_v = P_{\text{ref}} \exp \left[ -\frac{\Delta H_v}{R_g} \left( \frac{1}{T} - \frac{1}{T_{\text{ref}}} \right) \right]$ ,  $P_{\text{ref}}$  is 1 bar and  $T_{\text{ref}}$  is 3915 K from fits to data by Leideret al. [8]. The total power of radiation can be calculated by integrating Planck's radiation function over all wavelengths:

$$\dot{Q}_r = \int_0^\infty \varepsilon_{\lambda_{\text{LII}}} \frac{2\pi^2 D^2 h c^2}{\lambda_{\text{LII}}^5 \left[ \exp \left( \frac{hc}{\lambda_{\text{LII}} k_B T} \right) - 1 \right]} d\lambda_{\text{LII}} \quad (7)$$

where  $h$  is Planck's constant,  $c$  is the speed of light, and  $k_B$  is the Boltzmann constant. According to Kirchhoff's law [9,10], absorptivity equates with emissivity, and the emissivity for particles in the Rayleigh

limit [3]  $\varepsilon_{\lambda_{\text{LII}}}$  is assumed to be:  $\varepsilon_{\lambda_{\text{LII}}} = \frac{4\pi D E(m)}{\lambda_{\text{LII}}}$

By combining Eqs. (1) to (7), the differential equation Eq. (1) can be solved numerically with certain initial condition of  $D = D_0$  and  $T = T_g$  to obtain  $T(t)$ . The values used for all relevant variables values are collected on Table 1 :

**Table 1. Values for model calculations.**

	Units	Value
$\Delta H_v$	J/mol	$7.78 \times 10^5$ at 3915 K [1]
$W_s$	kg/mol	0.01201
$\rho_s$	kg/m <sup>3</sup>	$2303.1 - 7.3106 \times 10^{-5} T$ [11–13]
$c_s$	J/kg·K	$1878 + 0.1082 T - 151.49 T^{-2}$ [7]
$\alpha_T$	-	0.3 [3,11]
$k_a$	W/m·K	$5.83 \times 10^7 (T_g / 273)^{0.82}$ [1]

The LII signal  $S_{\text{LII}}$  at a specific emission wavelength  $\lambda_{\text{LII}}$  is calculated according to Planck's radiation function:

$$S_{\text{LII}}(t) = \frac{8\pi^3 hc^2 E(m) D^3}{\lambda^6} \left[ \frac{1}{\exp\left(\frac{hc}{\lambda k_B T(t)}\right) - 1} - \frac{1}{\exp\left(\frac{hc}{\lambda k_B T_g}\right) - 1} \right] \quad (8)$$

For a certain particle diameter distribution PDF( $D$ ), assuming that the particle number concentration  $n_p$  is constant in the probe volume  $V_m$  during a single LII event, an integration considering the particle size distribution function PDF( $D$ ) yields the total LII signal  $J_{\text{LII}}(t)$  at the detector surface at time  $t$ :

$$J_{\text{LII}}(t) = C_{\text{det}} n_p V_m \int_0^{\infty} \text{PDF}(D) S_{\text{LII}}(t) dD \quad (9)$$

where  $C_{\text{det}}$  is a constant of the detection system.

Previous study shows that the decay of  $J_{\text{LII}}(t)$  is dominated by Sauter mean diameters  $D_{32}$  [14,15] since the surface heat conduction is the dominating term in Eq. (1).  $D_{32}$  is defined as:

$$D_{32} = \frac{\int_0^{\infty} D^3 \text{PDF}(D) dD}{\int_0^{\infty} D^2 \text{PDF}(D) dD} \quad (10)$$

This means the different particles distributions share a same  $D_{32}$  will produce similar  $J_{\text{LII}}(t)$  decay curve. For simplicity, we use a uniform particle distribution with a certain  $D_{32}$  in Eq. (9) to replace the integration term and obtain:

$$J_1(D_{32}) = C_{\text{det}} n_p V_m S_{\text{LII}}(t, D_{32}) \quad (11)$$

In the present study, we use the model described above to estimate the LII signal collected by ICCD cameras in the first 50 ns and second 50 ns for a group of particles with certain  $D_{32}$ , which are denoted with  $J_1(D_{32})$  and  $J_2(D_{32})$  respectively. Thus we have:

$$\begin{cases} J_1(D_{32}) = \int_0^{50(\text{ns})} J_{\text{LII}}(t, D_{32}) dt \\ J_2(D_{32}) = \int_{50(\text{ns})}^{100(\text{ns})} J_{\text{LII}}(t, D_{32}) dt \end{cases} \quad (12)$$

The value of the ratio of the  $J_1(D_{32})$  and  $J_2(D_{32})$  can be calculated and used to in the LIF image correction. The experimental parameters inputted into the calculation are shown in Table 2:

**Table 2. Experimental parameters inputted into the calculation.**

Parameter	Value
FWHM of laser pulse	5 ns
Laser fluence $F$	450 J/m <sup>2</sup>
Laser wavelength $\lambda_l$	266 nm
Detection wavelength $\lambda$	330, 360, 390, 525 nm
Gas temperature $T_g$	1750 K

For a given group of particle within a problem volume with a certain  $D_{32}=20$  nm, the calculated LII signal is shown in Fig. 1.

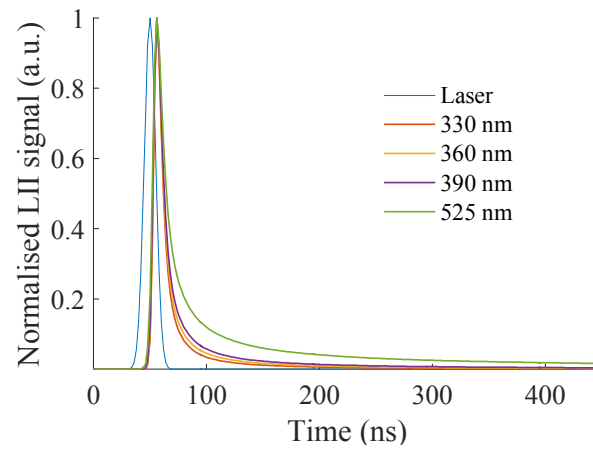


**Figure 1. The calculated LII response of a given uniform soot particle distribution  $D_{32}=20$  nm with input parameters shown in table 1.**

The correction coefficient  $K(D_{32}) = J_1(D_{32}) / J_2(D_{32})$  of 330, 360, 390, 525 nm is calculate and plotted against  $D_{32}$  in Fig. 2.

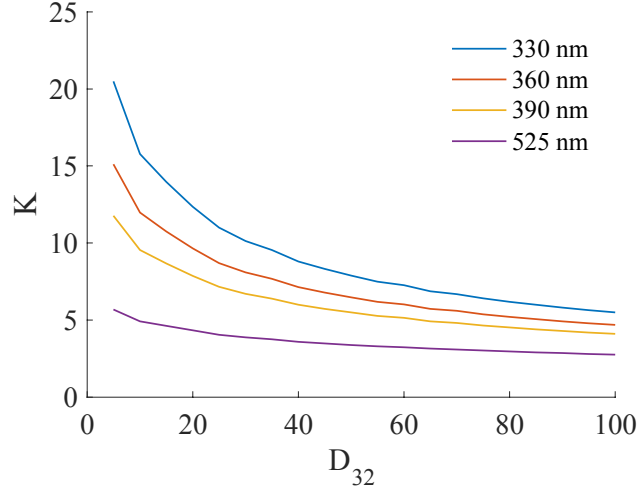


**Figure 2. Calculated correction coefficient  $K$  against  $D_{32}$ .**

The value of  $D_{32}$  across the tested flames can be evaluated in our previous publication [16], thus the value of  $K$  can then be determined with Fig. 2. Then, by using Eq. (13), the LIF signal  $S_{\text{LIF,cor}}$  can be corrected.

$$S_{\text{LIF,cor}} = S_{\text{LIF}} - K \cdot J_2 \quad (13)$$

For an example, the  $D_{32}$  values is 12.84 nm at 1.2 cm, 46.08 nm at 1.3 cm, 55.3 nm at 1.4 cm, and 81.44 at 1.5 cm for the flame L1 case in [16]. The  $K$  value converges to a constant starting from 50 nm, as shown in Fig. 2. Given that the experimental signal values are abstracted from HABs = 1.4 to HABs = 2.0 cm, the  $D_{32}$  value is assumed to be 80 nm in present study.

## References:

- [1] Melton LA. Soot diagnostic based on laser heating. *Appl Opt* 1984;23:2201–8.
- [2] Schulz C, Kock BF, Hofmann M, Michelsen H, Will S, Bougie B, et al. Laser-induced incandescence: recent trends and current questions. *Appl Phys B* 2006;83:333–54. doi:10.1007/s00340-006-2260-8.
- [3] Michelsen H a., Liu F, Kock BF, Bladh H, Boiarciuc a., Charwath M, et al. Modeling laser-induced incandescence of soot: a summary and comparison of LII models. *Appl Phys B* 2007;87:503–21. doi:10.1007/s00340-007-2619-5.
- [4] Michelsen H a., Schulz C, Smallwood GJ, Will S. Laser-induced incandescence: Particulate diagnostics for combustion, atmospheric, and industrial applications. *Prog Energy Combust Sci* 2015:1–47. doi:10.1016/j.pecs.2015.07.001.
- [5] Krishnan SS, Lin K-C, Faeth GM. Extinction and Scattering Properties of Soot Emitted From Buoyant Turbulent Diffusion Flames. *J Heat Transfer* 2001;123:331. doi:10.1115/1.1350823.
- [6] Snelling DR, Liu F, Smallwood GJ, Gülder ÖL. Determination of the soot absorption function and thermal accommodation coefficient using low-fluence LII in a laminar coflow ethylene diffusion flame. *Combust Flame* 2004;136:180–90. doi:10.1016/j.combustflame.2003.09.013.
- [7] Kock B, Tribalet B, Schulz C, Roth P. Two-color time-resolved LII applied to soot particle sizing in the cylinder of a Diesel engine. *Combust Flame* 2006;147:79–92. doi:10.1016/j.combustflame.2006.07.009.
- [8] Leider HR, Krikorian OH, Young D a. Thermodynamic properties of carbon up to the critical point. *Carbon N Y* 1973;11:555–63.



- [9] De Iuliis S, Migliorini F, Cignoli F, Zizak G. Peak soot temperature in laser-induced incandescence measurements. *Appl Phys B* 2006;83:397–402. doi:10.1007/s00340-006-2210-5.
- [10] De Iuliis S, Migliorini F, Cignoli F, Zizak G. 2D soot volume fraction imaging in an ethylene diffusion flame by two-color laser-induced incandescence (2C-LII) technique and comparison with results from other optical diagnostics. *Proc Combust Inst* 2007;31:869–76. doi:10.1016/j.proci.2006.07.149.
- [11] Bladh H, Johnsson J, Bengtsson P-E. On the dependence of the laser-induced incandescence (LII) signal on soot volume fraction for variations in particle size. *Appl Phys B* 2007;90:109–25. doi:10.1007/s00340-007-2826-0.
- [12] Blacha T, Di Domenico M, Gerlinger P, Aigner M. Soot predictions in premixed and non-premixed laminar flames using a sectional approach for PAHs and soot. *Combust Flame* 2012;159:181–93. doi:10.1016/j.combustflame.2011.07.006.
- [13] Olofsson N-E, Johnsson J, Bladh H, Bengtsson P-E. Soot sublimation studies in a premixed flat flame using laser-induced incandescence (LII) and elastic light scattering (ELS). *Appl Phys B* 2013;112:333–42. doi:10.1007/s00340-013-5509-z.
- [14] Sipkens T a., Mansmann R, Daun KJ, Petermann N, Titantah JT, Karttunen M, et al. In situ nanoparticle size measurements of gas-borne silicon nanoparticles by time-resolved laser-induced incandescence. *Appl Phys B Lasers Opt* 2013;1–14. doi:10.1007/s00340-013-5745-2.
- [15] Liu F, Stagg BJ, Snelling DR, Smallwood GJ. Effects of primary soot particle size distribution on the temperature of soot particles heated by a nanosecond pulsed laser in an atmospheric laminar diffusion flame. *Int J Heat Mass Transf* 2006;49:777–88. doi:10.1016/j.ijheatmasstransfer.2005.07.041.

- [16] Gu C, Lin H, Camacho J, Lin B, Shao C, Li R, et al. Particle size distribution of nascent soot in lightly and heavily sooting premixed ethylene flames. *Combust Flame* 2016;165:177–87.  
doi:10.1016/j.combustflame.2015.12.002.